Estimation of future changes in photovoltaic potential in Australia due to climate change

Shukla Poddar[1], Jason Peter Evans[1], Merlinde J. Kay[1], Abhnil Amtesh Prasad[2], and Stephen Bremner[1]

[1]University of New South Wales
[2]The University of New South Wales

November 24, 2022

Abstract

Solar photovoltaic (PV) energy is one of the most preferred and fastest growing emission-free energy sources in Australia. However, the dependency of PV generation on climatological factors can impact future power generation. Considering the future large-scale deployment of PV systems, accurate climate information is essential for PV site selection, stable grid regulation, planning and energy output projections. In this study, the effect of projected changes in shortwave downwelling radiation, temperature and wind speed on the performance of PV systems over Australia is examined using regional climate projections. Results indicate a small, but significant decline in future PV potential over Australia due to reduced insolation and increased temperature. Under a high emission scenario, the cell temperature is predicted to increase 2.5°C by 2070 leading to increased periods of significantly reduced cell efficiency (6-13 days/year) mostly in Western and central Australia.

Estimation of future changes in photovoltaic potential in Australia due to climate change

Shukla Poddar[1,2], Jason P Evans[2,3], Merlinde Kay[1], Abhnil Prasad[1,2,3], Stephen Bremner[1]

[1]School of Photovoltaic and Renewable Energy Engineering, University of New South Wales, Sydney, Australia
[2]ARC Centre of Excellence for Climate Extremes, University of New South Wales, Sydney, Australia
[3] Climate Change Research Centre, Biological, Earth and Environmental Sciences, University of New South Wales, Sydney, Australia

Corresponding author: Shukla Poddar (s.poddar@unsw.edu.au)

Key Points:

- Ensemble mean of regional climate model simulations predict a decline in Photovoltaic (PV) potential over Australia by 2079.
- Projected changes in the temperature make the largest contribution to the future PV potential decline followed by changes in radiation.
- PV cell temperature is predicted to increase in the future enhancing the cell efficiency losses and reduction in generation.

Abstract

Solar photovoltaic (PV) energy is one of the most preferred and fastest growing emission-free energy sources in Australia. However, the dependency of PV generation on climatological factors can impact future power generation. Considering the future large-scale deployment of PV systems, accurate climate information is essential for PV site selection, stable grid regulation, planning and energy output projections. In this study, the effect of projected changes in shortwave downwelling radiation, temperature and wind speed on the performance of PV systems over Australia is examined using regional climate projections. Results indicate a small, but significant decline in future PV potential over Australia due to reduced insolation and increased temperature. Under a high emission scenario, the cell temperature is predicted to increase 2.5°C by 2070 leading to increased periods of significantly reduced cell efficiency (6-13 days/year) mostly in Western and central Australia.

Plain Language Summary

Solar PV is an established and fastest growing renewable technology in Australia to combat global warming and carbon emissions. PV power generation is affected by climatological factors like radiation, temperature, wind speed, clouds, etc. making it susceptible to future climate change. Considering large scale investments in future PV plants, it is essential to investigate the potential impact of climate change on PV power generation at different time scales. This study assesses long-term changes in the future PV potential over Australia and the effects of projected changes in insolation, temperature and wind speed on PV power generation capacity for the near (2020-2039) and far-future (2060-2079) periods. PV potential is projected to decrease over Australia in the future due to elevated temperature and reduced insolation. On further investigation, we find that the cell temperatures are projected to increase in the future, resulting in increased degradation and risks of failure. The elevated cell temperatures significantly contribute to cell efficiency losses, that are expected to increase in the future indicating further reductions in PV power generation. Long-term PV power projections can help in understanding the variations in future power generation and identifying regions where PV systems will be highly susceptible to losses in Australia.

1. Introduction

With the high rate of global warming and enhanced greenhouse gas emissions, Australia has moved towards sustainable energy systems by deploying renewable technologies in the last decade. Almost 27.7% of Australia's electricity was generated from renewable energy in 2020 (Clean Energy Australia Report, 2021). Large-scale renewable energy generation capacity of almost 2 GW was added to the electricity grid in 2020, which includes an additional 893 MW of generation capacity in large-scale solar along with a 3GW capacity of rooftop Photovoltaic (PV). The solar PV capacity is expected to increase by 20 GW by 2026 and by another 72 GW by 2050 to meet the zero net emissions target (Energy Networks Australia, 2017). To achieve these targets, resource assessments and energy production forecasts at all timescales will be required during the planning, construction and operation phases of a solar plant (Crook et al., 2011), along with planning storage solutions for the variable electricity generation of PV systems.

Energy generated from PV technology at a site mainly depends on solar irradiance availability at that location and the PV cell temperatures. It has been found that for every 1°C rise in the cell temperature, the solar cell efficiency decreases by 0.5% (Kawajiri et al., 2011; Müller et al., 2019). The PV power output varies non-linearly with irradiance, especially at lower intensities (Müller et al., 2019). Climate variables like cloud cover, wind speed, aerosols and relative humidity (Pérez et al., 2019; Solaun & Cerdá, 2019) also affect PV production. Global solar irradiance is directly dependent on cloud cover and atmospheric conditions. The cloud cover pattern and precipitation distribution rates are likely to change in the future under different warming scenarios (Collins et al., 2013; Moon & Ha, 2020). Dependency of PV power output on these meteorological factors introduce a large uncertainty for investments. Thus, mitigating risks for investments in future large-scale PV plants requires detailed future climate analysis, as well as financial analysis to determine the economic feasibility of a project.

Several studies to quantify the long-term changes in future PV power availability have been undertaken both globally as well as regionally using climate projections. Global studies based on coarse-resolution global simulations including the Coupled Model Intercomparison Project 3 & 5 (CMIP3 and CMIP5) (Crook et al., 2011; Wild et al., 2015) projections indicate little predicted changes in the PV production over Australia. Crook et al., 2011 investigated the future changes in CSP and PV productivity and have suggested an increase in PV productivity over Europe and China, a decrease over the USA and Saudi Arabia with a slight decline over Australia and Algeria by 2080. Wild et al., 2015 suggest that PV power may increase in Spain and Germany, decrease in North-India and North-West China with an almost negligible increase over Australia by 2049. None of these studies explicitly consider the additional impact of changes in cell temperatures. Regional studies, with both higher resolution regional model simulations and coarser resolution climate projection data, have been carried out for various parts of the world. These include studies for Europe (Jerez et al., 2015b using Euro-CORDEX simulations; Müller et al., 2019 using CMIP5 projections), Europe and Africa (Gaetani et al., 2014 using ECHAM5 model), Greece (Panagea et al., 2014 using five regional models), UK (Burnett et al., 2014 using UKCP09 probabilistic climate change projections), West Africa (Bazyomo et al., 2016 using CORDEX simulations for Africa).

Studies focusing on the Australian continent have focused more on historical time periods and highlighted the strong seasonal variability of global horizontal irradiance (GHI) and direct normal irradiance (DNI) (Prasad et al., 2015, 2017). The variability of GHI and DNI over Australia is directly influenced by the changes in cloud cover due to large-scale climate drivers (like El-Niño Southern Oscillation (ENSO), monsoon, and sub-tropical ridge) and synoptic features (like cloud bands, troughs, and fronts) (Prasad et al., 2015, 2017). Davy & Troccoli, 2012 analyzed the effects of ENSO and Indian Ocean Dipole (IOD) on solar radiation over Australia (for the period 1989-2008) and highlighted the variability in radiation patterns, especially during the winter period over the continent. Huang et al., 2020 have reported the temperature de-rating impacts on solar and wind farms for two sites in Australia. However, to date, an extensive regional study analyzing future energy projections from PV technology has not been attempted for Australia. Similarly, future changes in cell temperature due to climate change, are yet to have been incorporated. The objective of this work is to examine the future changes in PV power generation over Australia, and the role of climate variables in driving such changes. In this study, we also project the future cell temperature changes over Australia and examine its impact on future PV productivity.

2. Methods

2.1. NARCliM regional projections

Regional climate model (RCM) simulations from the New South Wales/Australian Capital Territory Regional Climate Modelling (NARCliM) project have been used in this study (Evans et al., 2014). The NARCliM projections consist of two spatial domains at ~50 Km (0.44°×0.44°, covering CORDEX-Australasia region) and ~10 Km (0.088°×0.088°) spatial resolution (covering south-east Australia) for three different time periods: present (1990-2009), near future (2020-2039) and far future (2060-2079). The future periods are forced using the A2 scenario following the Special Report on Emission Scenarios (SRES). The A2 scenario projects a surface warming of 3.4°C by 2100 (IPCC, 2007). The RCM ensembles have been created by downscaling the four global climate models (GCM) (MIROC3.2, ECHAM5, CCCMA3.1, and CSIRO-Mk3.0) using the weather research and forecasting (WRF) model version 3.3. These GCMs were chosen from CMIP3 according to their performance over the Australian domain, their ability to span potential future climate over South-East Australia and the independence of their errors (Evans et al., 2014). Three different RCM versions were created by combining different planetary boundary layer, cumulus and atmospheric radiation schemes (supplementary Table s1). The RCM configurations were selected from 36-member multi-physics ensemble based on their skill and independence of errors in a two-step selection process (Evans et al., 2012; Evans et al., 2014). Thus, each period consists of 12 ensemble members: 4 GCMs x 3 RCMs. The NARCliM ensemble has been extensively evaluated and found to reproduce many aspects of the regions climate including: the mean climatology (Olson et al., 2016); precipitation extremes (Evans et al. 2017); heatwaves (Gross et al., 2017); drought (Herold et al., 2018); and teleconnections with large-scale climate modes (Fita et al., 2016). All the analysis in this study has been done using the NARCliM three-hourly temperature, downward shortwave solar radiation and wind speed data.

2.2. Estimation of PV potential and cell efficiency

The power generated by a PV plant directly depends on the nominal installed capacity and the PV power generation potential of the location. PV potential characterizes the amount of solar energy retrieved at a location by a typical utility-scale PV system under ambient conditions. It is a dimensionless quantity that accounts explicitly for the performance of the PV cells to their nominal power capacity. Therefore, the instantaneous PV power of a site is the product of its PV potential and the nominal installed capacity. PV potential has been calculated using the general expression (Jerez et al., 2015a) in equation 1:

$$PV\ Potential\ (P) = \mathrm{P_R} \times {}^{\mathrm{G}}/_{\mathrm{G_{STC}}} \dots\dots\dots\dots\dots\dots eq\ 1$$

where, G is the downward shortwave solar radiation (W/m^2) and G_{STC} is G in standard test conditions (1000 W/m^2). P_R is the performance ratio of the PV cell accounting for all the losses due to increase in cell temperature. Estimation of the PV potential does not consider the tilt of the array. Note, spectrum effects on the PV power output is small (Huld & Gracia

Amillo, 2015) and has not been considered. The performance ratio of the PV cell is estimated (Mavromatakis et al., 2010; Davy & Troccoli, 2012) using equation 2:

$$P_R = 1 + \gamma\left(T_{cell} - T_{ref}\right) \dots \dots \dots \dots \dots \dots . eq\ 2$$

where γ = -0.005 (Jerez et al., 2015a). T_{cell} and T_{ref} denote cell temperature and reference temperature, respectively. The reference temperature is taken to be 25 ºC and T_{cell} is modelled according to Chenni et al., 2007.

$$T_{cell} = C_1 + C_2 T + C_3 G + C_4 V \dots \dots \dots \dots \dots \dots eq\ 3$$

where T is the air temperature around the cells (ºC), V is the wind speed (m/s) and C_1, C_2, C_3 and C_4 are coefficients of cell temperature that depend on the cell properties and affect the heat transfer of the cell. Representing a generalized cell, the values of C_1, C_2, C_3 and C_4 are taken as 4.3 ºC, 0.943, 0.028 ºC m^2 W^{-1} and -1.528 ºCs m^{-1} (Jerez et al., 2015a). At standard temperature and irradiance, the power production reaches the rated value.

Efficiency of a PV cell has been calculated using the following equation:

$$\eta c = \eta t\ [1 - \beta\left(T_{cell} - T_{ref}\right)] \dots\dots\dots\dots\dots\dots\ eq\ 4$$

where T_{cell} and T_{ref} are the cell temperature and reference temperature respectively. ηt is the rated power conversion efficiency of the solar cell at reference temperature. β is efficiency temperature coefficient (0.45%/°C) (Kaldellis et al., 2014; Makrides et al., 2012). The quantity ($T_{cell} - T_{ref}$) increases with cell temperature and consequently decreases efficiency.

2.3. Contribution of climate variables in PV potential change

Combining equation 2 and 3 with equation 1, the expression for PV potential can be rewritten as (supplementary section 2):

$$PV_{pot} = \alpha_1 + \alpha_2 G^2 + \alpha_3 GT + \alpha_4 GV \dots \dots \dots \dots \dots \dots eq\ 5$$

$\alpha_1 = 1.1035 \times 10^{-3}(\mathrm{W/m^2})^{-1}$, $\alpha_2 = -1.4 \times 10^{-7}(\mathrm{W/m^2})^{-2}$, $\alpha_3 = -4.715 \times 10^{-6}(\mathrm{W°C/m^2})^{-1}$ and $\alpha_4 = 7.64 \times 10^{-6}(\mathrm{W/ms})^{-1}$. The total change in PV potential due to each variable (obtained using Taylor expansion of equation 5) can be expressed as:

$$\Delta PV_{pot} = \Delta G(\alpha_1 + \alpha_2 \Delta G + 2\alpha_2 G + \alpha_3 T + \alpha_4 V) + \alpha_3 G \Delta T + \alpha_4 G \Delta V + \alpha_3 \Delta G \Delta T + \alpha_4 \Delta G \Delta V \ldots\ldots\ldots\ldots\ldots\ldots eq\ 6$$

ΔT, ΔG and ΔV are the changes in temperature, radiation and wind between the historical and the future period. Hence, PV potential change due to temperature alone can be obtained by using $\Delta G = \Delta V = 0$ in equation 6. Analogously, the change in PV potential due to the influence of changes in radiation or wind alone is obtained by considering $\Delta T = \Delta V = 0$ and $\Delta G = \Delta T = 0$ respectively in equation 6. This method has been previously adopted by (Jerez et al., 2015b; Sawadogo et al., 2020).

2.4. Significance test

The statistical significance of the results is examined with Student's t-test and presented following the convention of Tebaldi et al., 2011. For each grid point, each ensemble member is individually tested for significance using a Student's t-test. When less than 50% of the ensemble members show a significant change ($\alpha < 0.05$), it is denoted in color. These are areas where little change is likely. Grid points, where at least 50% of the ensemble members show a significant change and at least 75% of the significant members agree on the direction of change, are denoted by color and stippling. These are areas with high confidence in the future change. Grid points where at least 50% of the ensemble members show significant change with less than 75% of them agreeing on the direction of change is denoted in white. These are areas with low confidence in the future change.

3. Results and Discussions

3.1. Future projections of PV power output over Australia

To assess the climate change impacts on PV productivity over Australia, future changes in the PV potential between the historical period (1990-2009) and future periods, near future (2020-2039) and far future (2060-2079), have been estimated (figure 1b, 1c). Western and Northern Australia have the maximum potential for PV production (figure 1a). The overall PV potential over Australia declines in the future with respect to the historical period. During the near future period, the decline in potential over Southern Australia is almost negligible (~0.25%) while the Northern regions show almost a uniform decline (1-1.25%). However, during the far future period the PV potential declines further with a maximum decrease in the South-East of the continent (~2 %).

Crook et al., 2011 also suggested that Australia may experience very slight changes in the power produced by 2080 upon estimating the global relative PV power. They computed a decline in power over most of the continent, however the East and the South coast had an increase in relative power output (~2%) (figure 1e Crook et al., 2011), in contrast to our results. Crook et al., 2011 used only one model, HadGEM1 from CMIP3 using SRES A1B scenario, which is the likely reason for such a contradiction and provides an example of how relying on a single model provides a limited view of potential future changes. Similar disagreement is also evident from the results of Wild et al., 2015, where a negligible increase in PV power throughout Australia (<0.05%) with relatively higher values (0.05-0.1%) over North-Eastern Australia (focal region selected for study) is predicted by the end of 2049. Such differences are expected due to the coarser resolution GCMs from CMIP5 used in their study. RCMs introduce an added value to the simulations compared to the GCMs due to the inclusion of higher resolution spatial details and better representation of small-scale processes in parametrization schemes (Bartók et al., 2016). The specific physical parameterization schemes selected for the NARCliM configuration can also be considered as one of the causes for the difference in results.

3.2. Dependency of PV potential on climatological variables and sensitivity to climate change

PV power output is directly driven by meteorological conditions, and its drivers are likely to change in the future. The changes in PV potential is influenced by changes in downward shortwave radiation, temperature and wind speed. Estimation of the individual strength of the impacts of these parameters on PV power is required to fully understand predictions for future scenarios. Projected changes in radiation show a decline over Northern Australia and a negligible increase over Southern Australia during the near future (figure 2a). A further decline in radiation during the far future is expected over most of the continent except the coastal regions of Northern and Southern Australia. Since the PV power can be generated only during the daytime, the changes in temperature and wind speed are estimated for the daytime only (6 am-6 pm). Overall, daytime temperature is expected to increase throughout the continent for both periods (~1 ºC in the near future and ~2.7 ºC in far future) while only small changes (0-0.3 ms^{-1}) in wind speed are expected for the future periods. Strong positive changes (0.2-0.5 ms^{-1}) in the wind speed are expected near the coastal regions of Northern Australia in the far future. Winds produce a cooling effect on the panel by reducing the cell temperature and thus enhancing the power output (Kaldellis et al., 2014).

Figure 3 shows the net contribution of radiation, temperature and wind towards the future changes in PV potential, respectively. The changes in PV potential due to each of the variables is obtained by considering the change in future values of that variable with other variables set at historical values (see methods section 2.3). The ratio of the future PV potential change due to an individual variable to the net change in the future PV potential estimates the contribution of that variable to future PV potential change. Positive contribution by a variable implies an increase in the future PV output due to changes in that variable. Similarly, a negative contribution implies a reduction in the future PV output due to a variable. This analysis reveals that future changes in PV potential over Australia are driven by the changes in temperature followed by radiation and wind respectively.

The negative contributions of temperature (figure 3b, e) towards the future PV potential change indicates that increases in temperature over Australia contributes towards the decline in PV potential (supplementary figure s2b, e). This highlights the sensitivity of PV cells to temperature consistent with the previous studies (Dubey et al., 2013; Radziemska, 2003). The change in PV potential due to radiation is negative near Northern Australia, negligible near central Australia and positive near Southern Australia (supplementary figure s2a) for the near future period. During the far future period, these changes due to radiation are negative throughout the continent except along the Northern and Southern coast where we see positive changes. The total PV potential change during the future periods exhibits small positive values mostly due to the positive contributions by radiation. Small positive contributions of wind speed to future PV potential change can be noted as opposed to large contributions of radiation and temperature. This is due to the small changes in future wind speed (figure 2c, f). The presence of cross-products makes it difficult to isolate the contributions by the individual variables and adds a negligible residual contribution.

3.3. Changes in the cell temperature and efficiency loss in future

Reliability of cell temperature on the atmospheric conditions makes it susceptible to changes according to the variations in climatic conditions. The performance of the PV modules decreases at high cell temperature due to cell efficiency losses. Thus, periods of high cell temperature can lead to significant decreases in the power generated (Dubey et al., 2013). The mean daily maximum cell temperature over Australia varies from 35-55 °C (figure 4a) for the historical period. Northern Australia records the highest mean daily maximum cell temperature (~55 °C). During the historical period, the highest recorded cell temperature varies from 55-72

°C (figure 4d). The highest cell temperature for the historical period is found in Northern Australia (72 °C) with relatively lower values along the Southern coastal regions (55-60 °C). Figure 4b, c depicts the projected changes in mean daily maximum cell temperature over Australia for the near future and far future period. Even though the mean daily maximum cell temperature is highest over Northern Australia (~55 °C), it is worth noting that the maximum rise in cell temperature is expected along the Eastern coast and Western Australia for both near future (~1 °C) and far future (~2.5 °C) periods. A similar increase in the mean cell temperature is also observed (supplementary figure s3). The results also indicate that the highest recorded cell temperature increases during the future period (Figure 4e, 4f). The maximum cell temperature for the near future period records ~1 °C rise uniformly except for parts of central Australia where an increase of 3-4 °C can be noted (Figure 4e). The increase in the highest cell temperature for the far future is higher (~6-7 °C) and fairly uniform throughout the continent unlike the near future period. It is worth noting that prolonged exposure to high cell temperatures can cause module degradation and enhance failure rates (Ndiaye et al., 2013; Omazic et al., 2019). Such considerations are beyond the scope of this study.

During the historical period with relatively high cell temperatures, the minimum annual cell efficiency over Australia is found to be 82-83% of the rated power conversion efficiency indicating a loss of 17-18% due to de-rating. De-rating is the reduction in power output of the PV cells from their rated power. It is important to note that this loss is expected to increase further in the future due to consistent increases in the cell temperature with a maximum annual loss of 19% and 21% in the near future and far future periods, respectively (supplementary figure s4). A similar increase in daily maximum relative cell efficiency loss is expected in the future (~0.5% and ~1.2% in near and far future respectively). Considering the possibility of future decline in relative cell efficiency due to elevated cell temperatures, it is useful to analyze the duration of expected loss per year and its future changes.

Beyond 58.33°C threshold cell temperature (supplementary section 3), a significant reduction in cell efficiency of at least 15% occurs. We therefore calculate the number of days/year when there will be expected loss in efficiency on reaching beyond the threshold cell temperature (figure 4 g-i). During the historical period, at least a 15% reduction in relative cell efficiency can be observed for 12-16 days/year in Northern and Central Australia. Results indicate that the maximum number of days/year above the threshold temperature increases for both near future (~2-4 days/year) and far future (~6-13 days/year) period. This indicates that the frequency of module efficiency degradation will increase in the future leading to a reduction in energy production. Furthermore, the periods of cell efficiency loss are consistent with the high cell temperature periods, imposing threats of power loss during these periods. A similar increase in the duration of 16-19% efficiency losses for both the future periods (supplementary figure s5) suggests an increased power loss by the end of the century across the country due to cell temperature rise. Increase in cell temperatures can lead to direct current (DC) to alternating current (AC) inverter de-rating and PV module de-rating (Huang et al., 2020). De-rating is one of the most significant impacts of temperature on power generation. It can negatively affect the supply-demand ratio causing power shortages, material damage along with a huge monetary loss to the industry (Ke et al., 2016).

4. Conclusion

This paper presents the expected changes in the future PV power potential over Australia under a high emission scenario using dynamically downscaled regional climate data from the NARCliM project. The PV potential is projected to decline during the 21st century over Australia for near future (2020-2039) and far future (2060-2079) period. The maximum decline in PV power generation is expected to occur in Northern Australia during the near future period and it decreases uniformly throughout the continent during the far future period with the highest expected decline in generation capacity in South-East Australia. The relative contributions of projected changes in temperature, downward solar radiation and wind speed on the future PV potential was analyzed. Results reveal that future changes in PV potential are determined primarily by the increase in temperature over Australia, with the next most significant effect being the projected decline in radiation. Elevated air temperatures due to global warming will induce higher cell temperatures over Australia, which leads to a decrease in relative cell efficiency and productivity. The expected number of days/year recording minimum 15% relative cell efficiency loss increases in the future. This indicates an increase in the number of days/year when PV power generated will be less than the rated generation capacity. PV systems are foreseen to largely expand over the 21st century in Australia, together with other technological developments. Future changes in PV power generation capacity should be considered when selecting locations and technology for transition to a low-carbon economy. These results can thus help in the assessment of resources and site allocation before deployment of large-scale projects in Australia.

Acknowledgements

The NARCliM regional climate projection data that support the findings of this study are available from the New South Wales government Climate Data Portal https://climatedata.environment.nsw.gov.au/. Analysis were conducted on the National Computational Infrastructure (NCI) facility based in Canberra, Australia.

Reference

Bartók, B., Wild, M., Folini, D., Lüthi, D., Kotlarski, S., Schär, C., Vautard, R., Jerez, S., & Imecs, Z. (2016). Projected changes in surface solar radiation in CMIP5 global climate models and in EURO-CORDEX regional climate models for Europe. *Climate Dynamics*, *49*(7–8), 2665–2683. https://doi.org/10.1007/s00382-016-3471-2

Bazyomo, S. D., Lawin, E., Coulibaly, O., & Ouedraogo, A. (2016). Forecasted changes in West Africa photovoltaic energy output by 2045. *Climate*, *4*(4), 1–15. https://doi.org/10.3390/cli4040053

Burnett, D., Barbour, E., & Harrison, G. P. (2014). The UK solar energy resource and the impact of climate change. *Renewable Energy*, *71*, 333–343. https://doi.org/10.1016/j.renene.2014.05.034

Chenni, R., Makhlouf, M., Kerbache, T., & Bouzid, A. (2007). A detailed modeling method for photovoltaic cells. *Energy*, *32*(9), 1724–1730. https://doi.org/10.1016/j.energy.2006.12.006

Clean Energy Australia Report. (2021). https://assets.cleanenergycouncil.org.au/documents/resources/reports/clean-energy-australia/clean-energy-australia-report-2021.pdf

Collins, M., Knutti, R., Arblaster, J., Dufresne, J.-L., Fichefet, T., Friedlingstein, P., Gao, X., Gutowski, W. J., Johns, T., Krinner, G., Shongwe, M., Tebaldi, C., Weaver, A. J., & Wehner, M. (2013). Long-term climate change: Projections, commitments and irreversibility. *Climate Change 2013 the Physical Science Basis: Working Group I Contribution to the Fifth Assessment Report of the Intergovernmental Panel on Climate Change*, *9781107057*, 1029–1136. https://doi.org/10.1017/CBO9781107415324.024

Crook, J. A., Jones, L. A., Forster, P. M., & Crook, R. (2011). Climate change impacts on future photovoltaic and concentrated solar power energy output. *Energy and Environmental Science*, *4*(9), 3101–3109. https://doi.org/10.1039/c1ee01495a

Davy, R. J., & Troccoli, A. (2012). Interannual variability of solar energy generation in

Australia. *Solar Energy*, *86*(12), 3554–3560.https://doi.org/10.1016/j.solener.2011.12.004

Dubey, S., Sarvaiya, J. N., & Seshadri, B. (2013). Temperature dependent photovoltaic (PV) efficiency and its effect on PV production in the world - A review. *Energy Procedia*, *33*, 311–321. https://doi.org/10.1016/j.egypro.2013.05.072

Energy Networks Australia. (2017). *Electricity network transformation roadmap: final report*. Energy Networks Australia. https://doi.org/https://doi.org/APO-76068

Evans, J. P., Ji, F., Lee, C., Smith, P., Argüeso, D., & Fita, L. (2014). Design of a regional climate modelling projection ensemble experiment - NARCliM. *Geoscientific Model Development*, *7*(2), 621–629. https://doi.org/10.5194/gmd-7-621-2014

Evans, Jason P., Argueso, D., Olson, R., & Di Luca, A. (2017). Bias-corrected regional climate projections of extreme rainfall in south-east Australia. *Theoretical and Applied Climatology*, *130*(3–4), 1085–1098. https://doi.org/10.1007/s00704-016-1949-9

Evans, Jason P., Ekström, M., & Ji, F. (2012). Evaluating the performance of a WRF physics ensemble over South-East Australia. *Climate Dynamics*, *39*(6), 1241–1258. https://doi.org/10.1007/s00382-011-1244-5

Fita, L., Evans, J. P., Argüeso, D., King, A., & Liu, Y. (2016). Evaluation of the regional climate response in Australia to large-scale climate modes in the historical NARCliM simulations. *Climate Dynamics*, *49*(7–8), 2815–2829. https://doi.org/10.1007/s00382-016-3484-x

Gaetani, M., Huld, T., Vignati, E., Monforti-Ferrario, F., Dosio, A., & Raes, F. (2014). The near future availability of photovoltaic energy in Europe and Africa in climate-aerosol modeling experiments. *Renewable and Sustainable Energy Reviews*, *38*, 706–716. https://doi.org/10.1016/j.rser.2014.07.041

Gross, M. H., Alexander, L. V., Macadam, I., Green, D., & Evans, J. P. (2017). The representation of health-relevant heatwave characteristics in a Regional Climate Model ensemble for New South Wales and the Australian Capital Territory, Australia. *International Journal of Climatology*, *37*(3), 1195–1210. https://doi.org/10.1002/joc.4769

Herold, N., Ekström, M., Kala, J., Goldie, J., & Evans, J. P. (2018). Australian climate extremes in the 21st century according to a regional climate model ensemble:

Implications for health and agriculture. *Weather and Climate Extremes*, *20*(April), 54–68. https://doi.org/10.1016/j.wace.2018.01.001

Huang, J., Jones, B., Thatcher, M., & Landsberg, J. (2020). Temperature impacts on utility-scale solar photovoltaic and wind power generation output over Australia under RCP 8.5. *Journal of Renewable and Sustainable Energy*, *12*(4). https://doi.org/10.1063/5.0012711

Huld, T., & Gracia Amillo, A. M. (2015). Estimating PV module performance over large geographical regions: The role of irradiance, air temperature, wind speed and solar spectrum. *Energies*, *8*(6), 5159–5181. https://doi.org/10.3390/en8065159

IPCC. (2007). *Climate Change 2007: Synthesis Report. Contribution of Working Groups I, II and III to the Fourth Assess- ment Report of the Intergovernmental Panel on Climate Change [Core Writing Team, Pachauri, R.K and Reisinger, A. (eds.)]. IPCC, Geneva, Switzerland,*. https://doi.org/10.1038/446727a

Jerez, S., Thais, F., Tobin, I., Wild, M., Colette, A., Yiou, P., & Vautard, R. (2015a). The CLIMIX model: A tool to create and evaluate spatially-resolved scenarios of photovoltaic and wind power development. *Renewable and Sustainable Energy Reviews*, *42*, 1–15. https://doi.org/10.1016/j.rser.2014.09.041

Jerez, Sonia, Tobin, I., Vautard, R., Montávez, J. P., López-Romero, J. M., Thais, F., Bartok, B., Christensen, O. B., Colette, A., Déqué, M., Nikulin, G., Kotlarski, S., Van Meijgaard, E., Teichmann, C., & Wild, M. (2015b). The impact of climate change on photovoltaic power generation in Europe. *Nature Communications*, *6*. https://doi.org/10.1038/ncomms10014

Kaldellis, J. K., Kapsali, M., & Kavadias, K. A. (2014). Temperature and wind speed impact on the efficiency of PV installations. Experience obtained from outdoor measurements in Greece. *Renewable Energy*, *66*, 612–624. https://doi.org/10.1016/j.renene.2013.12.041

Kawajiri, K., Oozeki, T., & Genchi, Y. (2011). Effect of temperature on PV potential in the world. *Environmental Science and Technology*, *45*(20), 9030–9035. https://doi.org/10.1021/es200635x

Ke, X., Wu, D., Rice, J., Kintner-Meyer, M., & Lu, N. (2016). Quantifying impacts of heat waves on power grid operation. *Applied Energy*, *183*(December), 504–512. https://doi.org/10.1016/j.apenergy.2016.08.188

Makrides, G., Zinsser, B., Phinikarides, A., Schubert, M., & Georghiou, G. E. (2012). Temperature and thermal annealing effects on different photovoltaic technologies. *Renewable Energy*, *43*(June 2006), 407–417. https://doi.org/10.1016/j.renene.2011.11.046

Mavromatakis, F., Makrides, G., Georghiou, G., Pothrakis, A., Franghiadakis, Y., Drakakis, E., & Koudoumas, E. (2010). Modeling the photovoltaic potential of a site. *Renewable Energy*, *35*(7), 1387–1390. https://doi.org/10.1016/j.renene.2009.11.010

Moon, S., & Ha, K. J. (2020). Future changes in monsoon duration and precipitation using CMIP6. *Npj Climate and Atmospheric Science*, *3*(1), 1–7. https://doi.org/10.1038/s41612-020-00151-w

Müller, J., Folini, D., Wild, M., & Pfenninger, S. (2019). CMIP-5 models project photovoltaics are a no-regrets investment in Europe irrespective of climate change. *Energy*, *171*, 135–148. https://doi.org/10.1016/j.energy.2018.12.139

Ndiaye, A., Charki, A., Kobi, A., Kébé, C. M. F., Ndiaye, P. A., & Sambou, V. (2013). Degradations of silicon photovoltaic modules: A literature review. *Solar Energy*, *96*, 140–151. https://doi.org/10.1016/j.solener.2013.07.005

Olson, R., Evans, J. P., Di Luca, A., & Argüeso, D. (2016). The NARCliM project: Model agreement and significance of climate projections. *Climate Research*, *69*(3), 209–227. https://doi.org/10.3354/cr01403

Omazic, A., Oreski, G., Halwachs, M., Eder, G. C., Hirschl, C., Neumaier, L., Pinter, G., & Erceg, M. (2019). Relation between degradation of polymeric components in crystalline silicon PV module and climatic conditions: A literature review. *Solar Energy Materials and Solar Cells*, *192*(December 2018), 123–133. https://doi.org/10.1016/j.solmat.2018.12.027

Panagea, I. S., Tsanis, I. K., Koutroulis, A. G., & Grillakis, M. G. (2014). Climate change impact on photovoltaic energy output: The case of Greece. *Advances in Meteorology*, *2014*. https://doi.org/10.1155/2014/264506

Pérez, J. C., González, A., Díaz, J. P., Expósito, F. J., & Felipe, J. (2019). Climate change impact on future photovoltaic resource potential in an orographically complex archipelago, the Canary Islands. *Renewable Energy*, *133*, 749–759. https://doi.org/10.1016/j.renene.2018.10.077

Prasad, A. A., Taylor, R. A., & Kay, M. (2015). Assessment of direct normal irradiance and cloud connections using satellite data over Australia. *Applied Energy*, *143*, 301–311. https://doi.org/https://doi.org/10.1016/j.apenergy.2015.01.050

Prasad, A. A., Taylor, R. A., & Kay, M. (2017). Assessment of solar and wind resource synergy in Australia. *Applied Energy*, *190*, 354–367. https://doi.org/https://doi.org/10.1016/j.apenergy.2016.12.135

Radziemska, E. (2003). The effect of temperature on the power drop in crystalline silicon solar cells. *Renewable Energy*, *28*(1), 1–12. https://doi.org/https://doi.org/10.1016/S0960-1481(02)00015-0

Sawadogo, W., Reboita, M. S., Faye, A., da Rocha, R. P., Odoulami, R. C., Olusegun, C. F., Adeniyi, M. O., Abiodun, B. J., Sylla, M. B., Diallo, I., Coppola, E., & Giorgi, F. (2020). Current and future potential of solar and wind energy over Africa using the RegCM4 CORDEX-CORE ensemble. *Climate Dynamics*, *0123456789*. https://doi.org/10.1007/s00382-020-05377-1

Solaun, K., & Cerdá, E. (2019). Climate change impacts on renewable energy generation. A review of quantitative projections. *Renewable and Sustainable Energy Reviews*, *116*. https://doi.org/10.1016/j.rser.2019.109415

Tebaldi, C., Arblaster, J. M., & Knutti, R. (2011). Mapping model agreement on future climate projections. *Geophysical Research Letters*, *38*(23), 1–5. https://doi.org/10.1029/2011GL049863

Wild, M., Folini, D., Henschel, F., Fischer, N., & Müller, B. (2015). Projections of long-term changes in solar radiation based on CMIP5 climate models and their influence on energy yields of photovoltaic systems. *Solar Energy*, *116*, 12–24. https://doi.org/10.1016/j.solener.2015.03.039

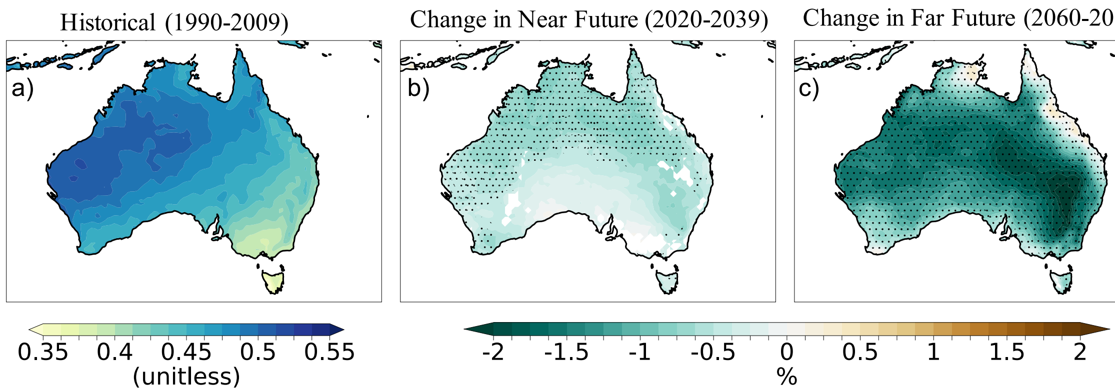

Figure 1. a) Historical PV potential. Relative percentage change in the PV potential over Australia for b) near future and c) far future period with respect to the historical period. Stippling indicates a significant change (according to method 2.4).

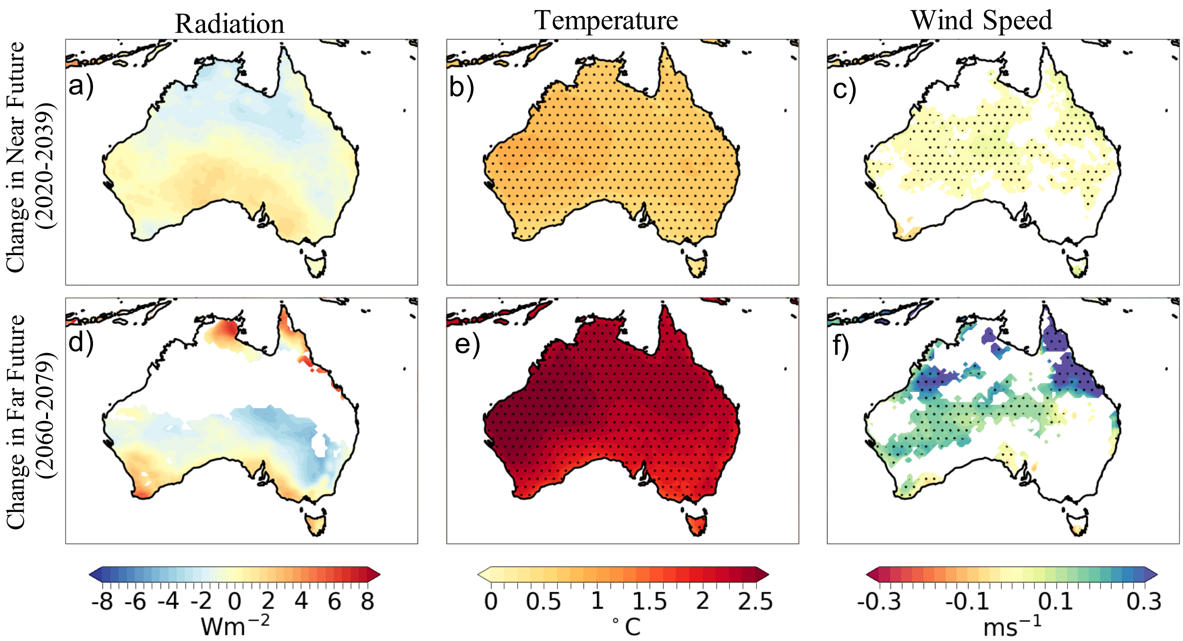

Figure 2. Change in the shortwave downward radiation (a, d), daytime temperature (b, e) and daytime wind speed (c, f) over Australia for the near future (a, b, c) and far future (d, e, f) period with respect to the historical period. Stippling indicates a significant change (according to method 2.4).

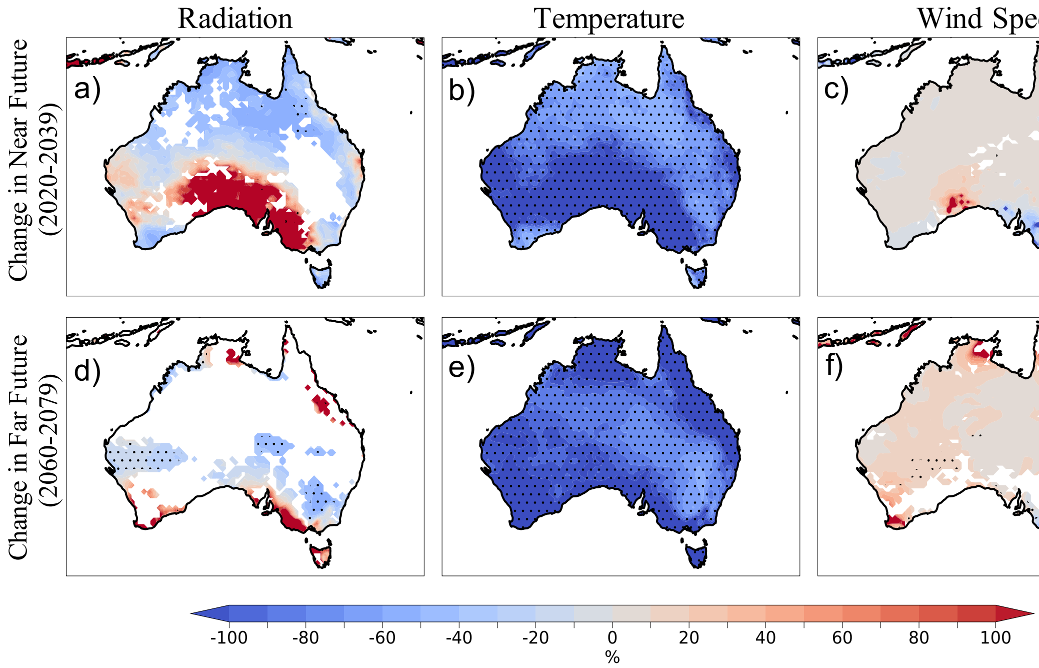

Figure 3. Contribution of meteorological variables to future PV potential change. Contribution by shortwave downward radiation (a, d), daytime temperature (b, e) and daytime wind speed (c, f) over Australia for the near future (a, b, c) and far future (d, e, f) period with respect to the historical period. Stippling indicates a significant change (according to method 2.4).

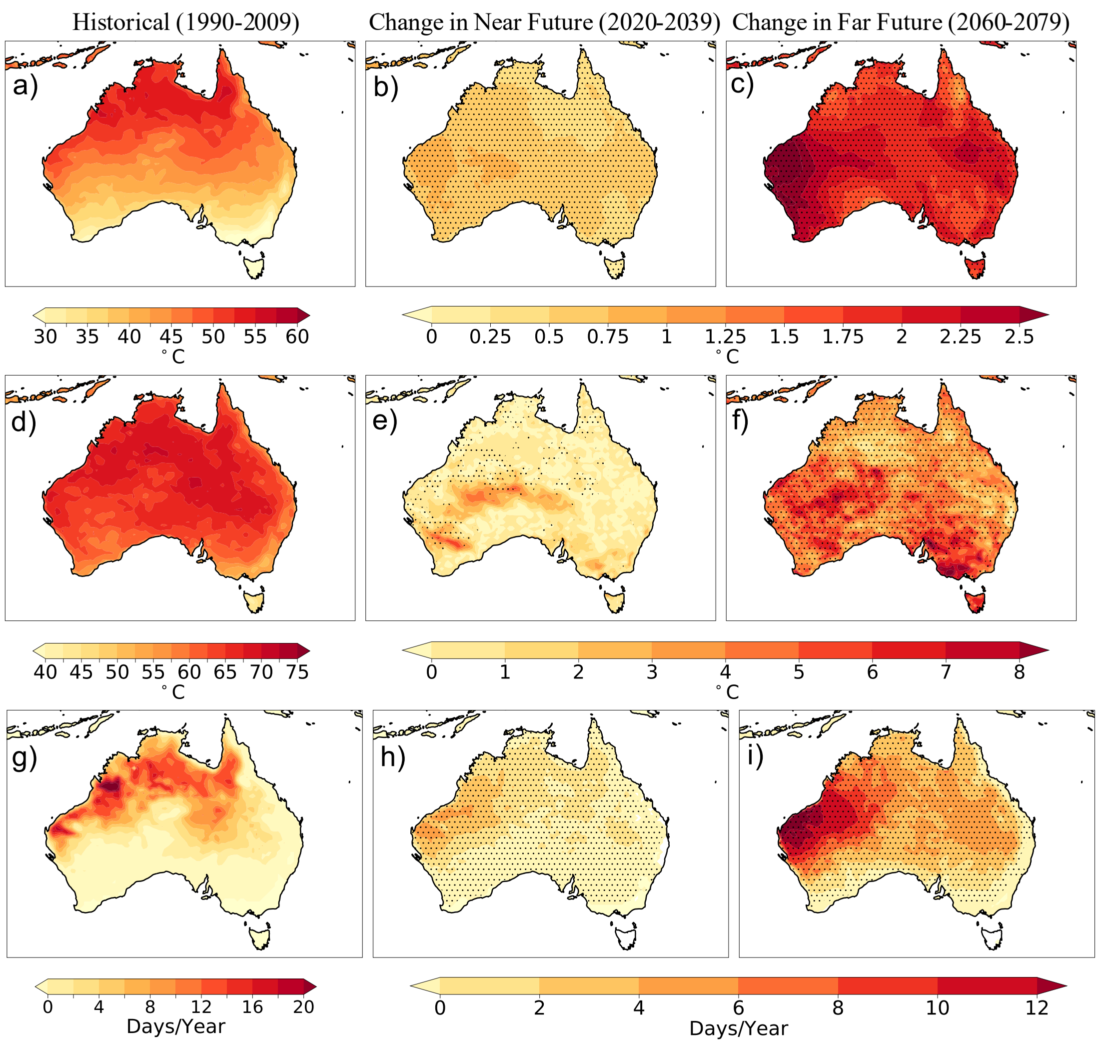

Figure 4. a) Mean daily maximum cell temperature over Australia for the historical period. Relative change in the mean daily maximum cell temperature for b) near future and c) far future period with respect to the historical period. d) Maximum cell temperature for the historical period. Relative change in the maximum cell temperature for e) near future and f) far future period with respect to the historical period. g) Climatological total number of days/year cell temperature exceeds the threshold temperature for minimum 15% reduction in relative cell efficiency for the historical period. Relative change in number of days/year the cell temperature exceeds the threshold temperature for minimum 15% reduction in relative cell efficiency for h) near future and i) far future period with respect to the historical period. Stippling indicates a significant change (according to method 2.4).

Supplementary for

Estimation of future changes in photovoltaic potential in Australia due to climate change

Shukla Poddar[1,2], Jason P Evans[2,3], Merlinde Kay[1], Abhnil Prasad[1,2,3], Stephen Bremner[1]

[1]School of Photovoltaic and Renewable Energy Engineering, University of New South Wales, Sydney, Australia

[2]ARC Centre of Excellence for Climate Extremes

[3]Climate Change Research Centre, Biological, Earth and Environmental Sciences, University of New South Wales, Sydney, Australia

Corresponding author: Shukla Poddar (s.poddar@unsw.edu.au)

Contents of this file

Table s1

Figures s1 to s5

Introduction

This supporting information includes:

- A table containing the details of the parameterization schemes used for creating different NARCliM ensemble members.
- Derivation of net change in PV potential due to contribution of radiation, temperature and wind speed.
- Cell efficiency loss threshold temperature.
- A figure representing the relationship of PV cell relative efficiency with irradiance, temperature and cell temperature (Figure s1).
- A figure representing the changes in the PV potential due to radiation, temperature and wind speed (Figure s2).
- A figure similar to figure 4(a-c) from the article demonstrating the mean cell temperature over Australia for the historical period and its changes for the near future and far future periods (Figure s3).
- A figure representing the cell efficiency losses for historical period and changes in the cell efficiency loss in the future periods (Figure s4).
- A figure similar to figure 4(g-i) from the article demonstrating the number of days/year there shall be a 16-19% efficiency loss during the historical period and the expected changes for the near and far future periods (Figure s5).

1. Parameterization schemes used for different ensemble members

***Table s1**: WRF schemes selected to generate the RCMs*

Ensemble Member	Planetary boundary layer physics/ surface layer physics	Cumulus physics	Microphysics	Shortwave/long-wave radiation physics	Land Surface
R1	MYJ /Eta similarity	Kain–Fritsch	WDM5	Dudhia/RRTM	Noah LSM
R2	MYJ /Eta similarity	Betts–Miller–Janjic	WDM5	Dudhia/RRTM	Noah LSM
R3	YSU/MM5 similarity	Kain–Fritsch	WDM5	CAM/CAM	Noah LSM

Table s1 describes the different parameterization schemes chosen to downscale four global climate models (GCMs) using three Weather Research Forecasting v3.3 (WRF) model configurations (Evans et al., 2014). The GCMs are chosen from the Coupled Model Intercomparison Project phase 3 (CMIP3) archive (MIROC3.2, ECHAM5, CCCMA3.1 and CSIRO-MK3.0). Thus the final ensemble contains 12 members (4 GCMs x 3 RCMs).

2. Contribution of climate variables in PV potential change

$$PV\ Potential\ (P) = P_R \times {}^{G}\!/_{G_{STC}} \ \ldots\ldots\ldots\ldots\ldots\ldots eq\ 1$$

where G_{STC}=1000 W/m^2

$$P_R = 1 + \gamma\left(T_{cell} - T_{ref}\right) \ldots\ldots\ldots\ldots\ldots\ldots eq\ 2$$

where T_{ref}= 25 °C

$$T_{cell} = C_1 + C_2T + C_3G + C_4V \ldots\ldots\ldots\ldots\ldots\ldots eq\ 3$$

where C_1, C_2, C_3 and C_4 are taken as 4.3 ºC, 0.943, 0.028 ºC m^2 W^{-1} and -1.528 ºCs m^{-1} respectively.

Combining equation 2 and 3 in 1,

$$P = 1 + \gamma\left((C_1 + C_2T + C_3G + C_4V) - T_{ref}\right) x \ {}^{G}\!/_{G_{STC}} \ \ldots\ldots\ldots\ldots\ldots\ldots eq\ 4$$

Adding values of G_{STC}, T_{ref}, γ, C_1, C_2, C_3 and C_4 to equation 4 we get,

$$PV_{pot} = \alpha_1 + \alpha_2G^2 + \alpha_3GT + \alpha_4GV \ldots\ldots\ldots\ldots\ldots\ldots eq\ 5$$

where $\alpha_1 = 1.1035 \times 10^{-3}(W/m^2)^{-1}$, $\alpha_2 = -1.4 \times 10^{-7}(W/m^2)^{-2}$, $\alpha_3 = -4.715 \times 10^{-6}$(W°C /m^2)$^{-1}$ and $\alpha_4 = 7.64 \times 10^{-6}(W/ms)^{-1}$

Using Taylor expansion in equation 5 we obtain the net change in PV potential due to radiation, temperature and wind speed,

$$\Delta PV_{pot} = \Delta G(\alpha_1 + \alpha_2\Delta G + 2\alpha_2G + \alpha_3T + \alpha_4V) + \alpha_3G\Delta T + \alpha_4G\Delta V + \alpha_3\Delta G\Delta T + \alpha_4\Delta G\Delta V \ldots\ldots\ldots\ldots\ldots\ldots eq\ 6$$

where ΔT, ΔG and ΔV are the changes in temperature, radiation and wind between the historical and the future period

The change in PV potential due to the change in radiation only is obtained from equation 6 (considering ΔT=ΔV=0):

$$\Delta PV_{pot_R} = \Delta G(\boldsymbol{\alpha}_1 + \alpha_2\Delta G + 2\alpha_2G + \alpha_3T + \alpha_4V) \ldots\ldots\ldots\ldots\ldots\ldots eq\ 7$$

The change in PV potential due to the change in temperature only is obtained from equation 6 (considering ΔG=ΔV=0):

$$\Delta PV_{pot_T} = \alpha_3 G \Delta \mathrm{T} \ldots\ldots\ldots\ldots\ldots\ldots eq\ 8$$

The change in PV potential due to the change in wind only is obtained from equation 6 (ΔT=ΔG =0):

$$\Delta PV_{pot_V} = \alpha_4 G \Delta \mathrm{V} \ldots\ldots\ldots\ldots\ldots\ldots eq\ 9$$

3. Cell efficiency loss threshold temperature

Cell efficiency is calculated using: $\eta c = \eta t\,[1 - \beta(T\_cell - T\_ref\,)]$ … … … … … … eq 10

where T_{cell} and T_{ref} are the cell temperature and reference temperature respectively. ηt is the rated power conversion efficiency of the solar cell at reference temperature. β is efficiency temperature coefficient (0.45%/°C) (Kaldellis et al., 2014; Makrides et al., 2012).

To estimate the cell efficiency loss of 15%, we find consider: $\frac{\eta t - \eta c}{\eta t} \times 100 = 15\%$.

On re-arranging the equation 10,

$$1 - \frac{\eta c}{\eta t} = 1 - [1 - \beta(T_{cell} - T_{ref})] \ldots\ldots\ldots\ldots\ \mathit{eq\ 11}$$

On adding all the values of the constants to equation 11, we can solve for T_{cell} = 58.33 °C for 15% loss. Similarly, threshold temperature is found to be 60.55 °C, 62.77 °C, 65 °C and 67.22 °C for 16%, 17% 18% and 19% loss respectively.

4. Relationship of PV cell relative efficiency with irradiance, temperature and cell temperature

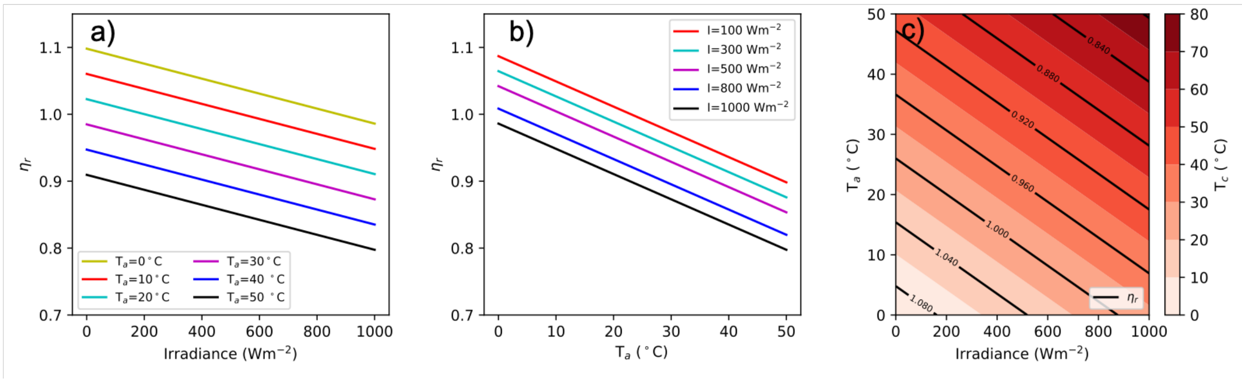

***Figure s1**. Relationship of relative efficiency with a) irradiance b) ambient temperature c) variation of cell temperature with irradiance and ambient air temperature.*

It can be noted that relative cell efficiency (η_r) decreases with an increase in ambient temperature at constant irradiance level. Cell temperature increases with an increase in the ambient temperature and irradiance. η_r also decreases with an increase in the cell temperature. There is an agreement with the previous literature (Chander et al., 2015; Notton et al., 2005) where they have reported similar relationship of relative cell efficiency with ambient temperature and irradiance.

5. Change in the net PV potential over Australia for the near future and far future periods due to radiation, temperature and wind speed

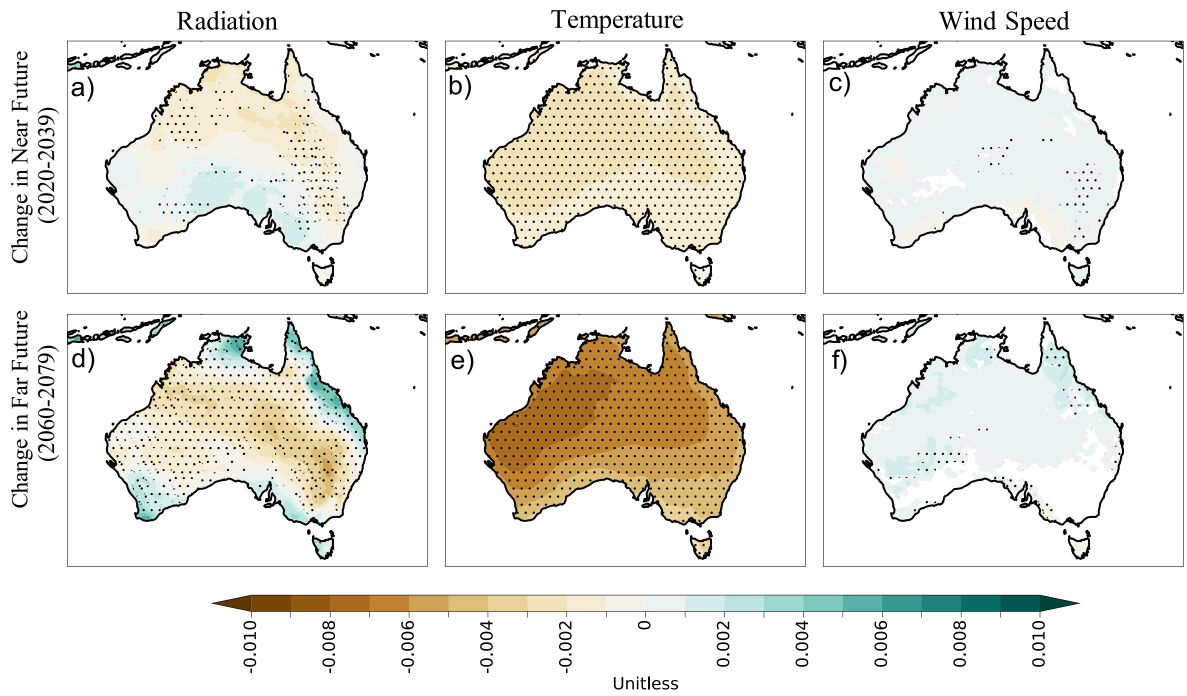

***Figure s2**. Change in future PV potential due to shortwave downward radiation (a, d), daytime temperature (b, e) and daytime wind speed (c, f) over Australia for near future (a, b, c) and far future (d, e, f) period with respect to the historical period. Stippling indicates significant change (according to method 2.4).*

The individual contribution by the climatological variables (shortwave downward radiation, temperature and wind speed) towards the future change in PV potential shows that temperature influences the PV potential maximum in Australia followed by radiation and wind speed. Positive changes in the PV potential due to radiation majorly contribute towards the net small positive PV potential change over Australia.

6. Mean cell temperature over Australia for the historical period and relative changes in the cell temperature for the future periods

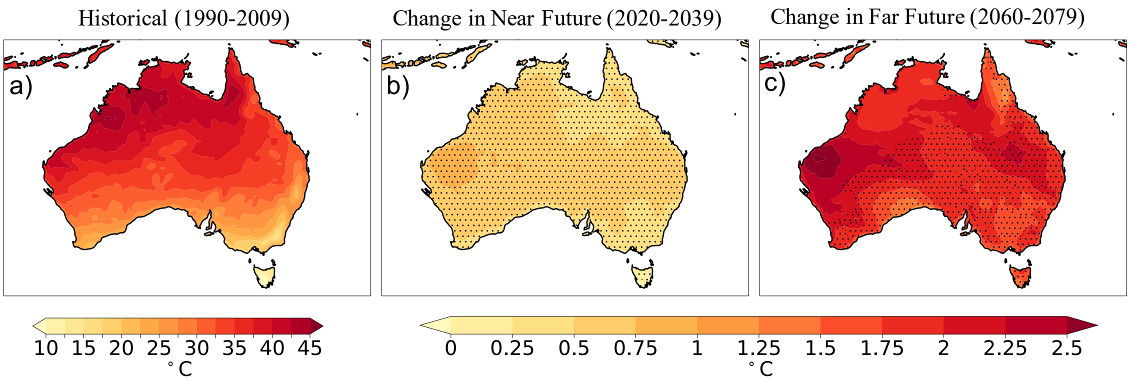

Figure s3 *a) Mean cell temperature over Australia for historical (1990-2009) period. Relative change in the mean cell temperature over Australia for b) near future (2020-2039) and c) far future (2060-2079) period with respect to the historical (1990-2009) period. Stippling indicates significant change (according to method 2.4).*

Australia records a mean cell temperature of around ~40-45 °C near the Northern Australia during the historical period. This mean cell temperature uniformly decreases (by ~5-10 °C) on moving towards the South of the continent. Due to climate change, an increase in around ~0.75-1 °C is expected during the near future period. Similar uniform rise in cell temperature (~1.5-2.5 °C) is expected for the far future period. The highest rise in the mean cell temperature is expected near the western part of the continent.

7. Cell efficiency loss

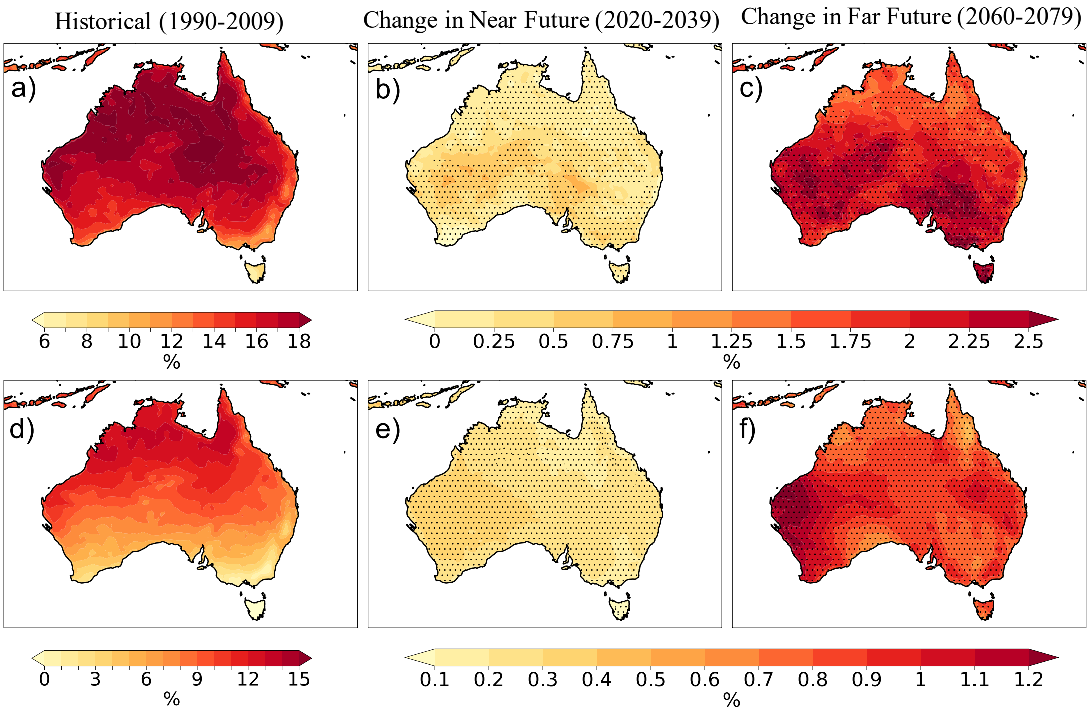

Figure s4*. a) Annual maximum relative cell efficiency loss for historical (1990-2009) period. Change in the relative cell efficiency over Australia for b) near future (2020-2039) and c) far future (2060-2079) period with respect to the historical (1990-2009) period. d) Daily maximum relative cell efficiency loss for historical (1990-2009) period. Change in the daily maximum relative cell efficiency over Australia for b) near future (2020-2039) and c) far future (2060-2079) period with respect to the historical (1990-2009) period. Stippling indicates significant change (according to method 2.4).*

The annual maximum relative cell efficiency loss over Australia for the historical period is maximum over the Northern part of the continent with values going up to 17-18%. This loss increases during the near future period by ~1% and further increases by 2-2.5% during the far future period. Similar changes in the daily maximum relative cell efficiency loss are expected in the future periods. This loss increases during the near future and far future periods by 0.5% and 1.2% respectively.

8. Changes in the cell efficiency due to high cell temperature in future

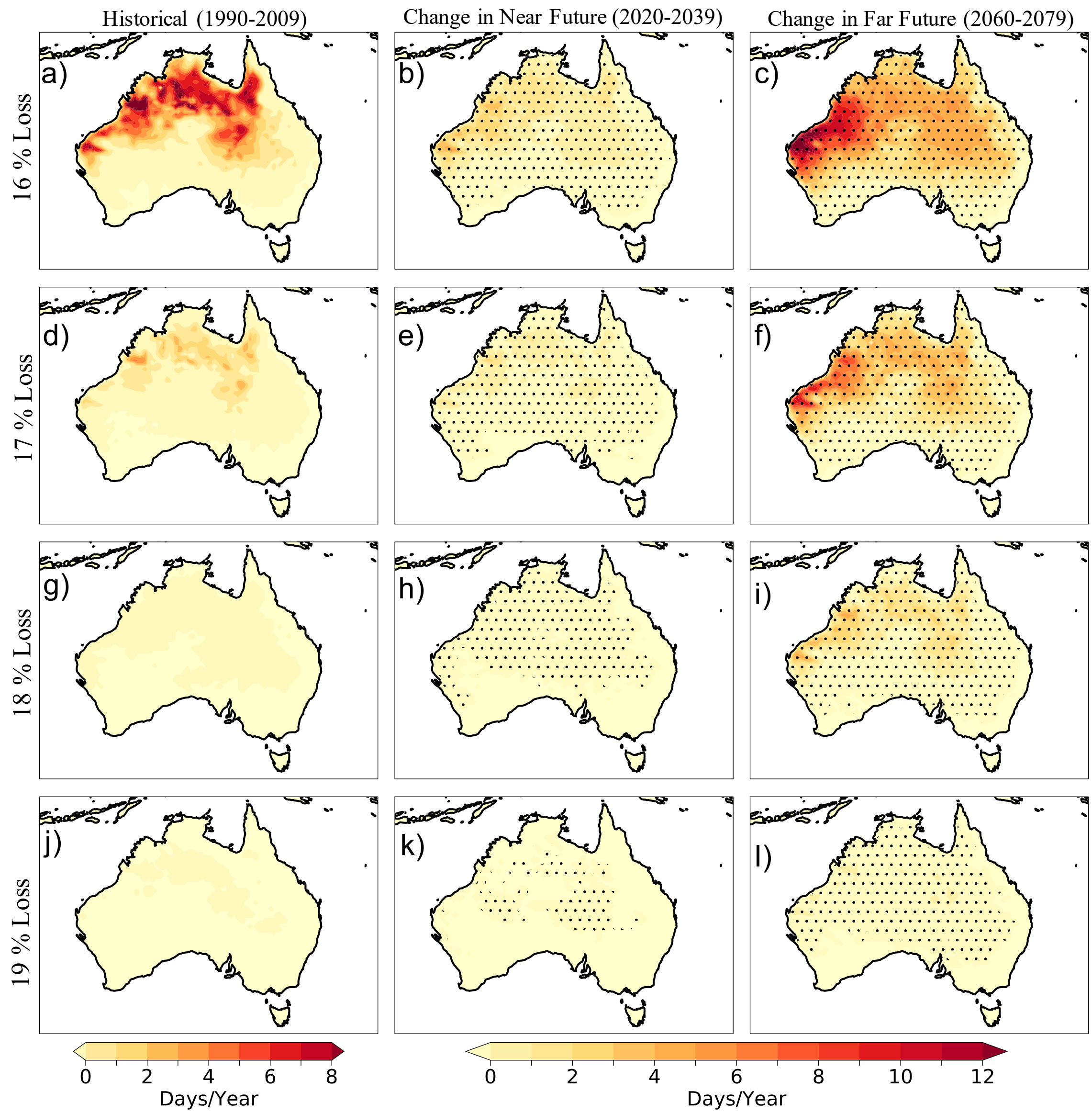

Figure s5. *Number of days/year cell temperature remains beyond threshold temperature for estimated loss in efficiency and there changes in the future periods.*

Reference

Chander, S., Purohit, A., Sharma, A., Arvind, Nehra, S. P., & Dhaka, M. S. (2015). A study on photovoltaic parameters of mono-crystalline silicon solar cell with cell temperature. *Energy Reports*, *1*, 104–109. https://doi.org/10.1016/j.egyr.2015.03.004

Evans, J. P., Ji, F., Lee, C., Smith, P., Argüeso, D., & Fita, L. (2014). Design of a regional climate modelling projection ensemble experiment - NARCliM. *Geoscientific Model Development*, *7*(2), 621–629. https://doi.org/10.5194/gmd-7-621-2014

Kaldellis, J. K., Kapsali, M., & Kavadias, K. A. (2014). Temperature and wind speed impact on the efficiency of PV installations. Experience obtained from outdoor measurements in Greece. *Renewable Energy*, *66*, 612–624. https://doi.org/10.1016/j.renene.2013.12.041

Makrides, G., Zinsser, B., Phinikarides, A., Schubert, M., & Georghiou, G. E. (2012). Temperature and thermal annealing effects on different photovoltaic technologies. *Renewable Energy*, *43*(June 2006), 407–417. https://doi.org/10.1016/j.renene.2011.11.046

Notton, G., Cristofari, C., Mattei, M., & Poggi, P. (2005). Modelling of a double-glass photovoltaic module using finite differences. *Applied Thermal Engineering*, *25*(17–18), 2854–2877. https://doi.org/10.1016/j.applthermaleng.2005.02.008